Dielectric Relaxation by Quantum Critical Magnons

Daniel Flavián,[1] Pavel A. Volkov,[2,3,4] S. Hayashida,[1,*] K. Yu. Povarov,[1,†] S. Gvasaliya,[1] Premala Chandra,[4] and A. Zheludev[1]

[1]*Laboratory for Solid State Physics, ETH Zürich, 8093 Zürich, Switzerland*
[2]*Department of Physics, Harvard University, Cambridge, Massachusetts 02138, USA*
[3]*Department of Physics, University of Connecticut, Storrs, Connecticut 06269, USA*
[4]*Department of Physics and Astronomy, Center for Materials Theory, Rutgers University, Piscataway, New Jersey 08854, USA*

(Received 9 February 2023; revised 2 April 2023; accepted 1 May 2023; published 26 May 2023)

We report the experimental observation of dielectric relaxation by quantum critical magnons. Complex capacitance measurements reveal a dissipative feature with a temperature-dependent amplitude due to low-energy lattice excitations and an activation behavior of the relaxation time. The activation energy softens close to a field-tuned magnetic quantum critical point at $H = H_c$ and follows single-magnon energy for $H > H_c$, showing its magnetic origin. Our study demonstrates the electrical activity of coupled low-energy spin and lattice excitations, an example of quantum multiferroic behavior.

DOI: 10.1103/PhysRevLett.130.216501

Magnetic insulators have long served as experimental prototypes for fundamental studies of thermal and quantum phase transitions. These materials can often be carefully tuned to quantum critical points (QCPs), for example by an applied magnetic field. In this category are soft-magnon and saturation transitions in antiferromagnets (AFs), often described in terms of a BEC of magnons [1–5]. In some real materials, magnetoelectric coupling results in dielectric anomalies at these magnetic-field-controlled transitions [6–11]. In most known examples, the electric polarization is merely a passive participant, reflecting the evolution of spin correlations; the latter is adequately described by purely magnetic microscopic Hamiltonians. There is no reason for this to always be the case. The search for qualitatively new dielectric phenomena at magnetic QCPs and the so-called "multiferroic" quantum critical regime [12] continues.

In this Letter, we present one such phenomenon, namely dipolar relaxation induced by magnons tuned through a magnetic-field-controlled QCP in the quantum spin system $Cs_2Cu_2Mo_3O_{12}$. This relaxation manifests itself as a frequency-dependent dielectric anomaly with a characteristic temperature scale distinct from both the classical transition temperature and the magnon Zeeman gap. We show that the anomaly is well-described by a relaxation model with a field-independent background dielectric constant attributed to lattice degrees of freedom alone. However, the relaxation time has an activated behavior with an *energy barrier closely following the single-magnon energy*. We conclude that the observed anomaly arises as a result of the interaction between low-energy lattice and quantum-critical spin degrees of freedom.

Our subject of study, $Cs_2Cu_2Mo_3O_{12}$, has previously attracted attention as a frustrated ferro-antiferro $S = 1/2$ quantum spin chain system [13,14]. It is structurally similar [15] to the more extensively studied $Rb_2Cu_2Mo_3O_{12}$ [11,13,22–25]. The Cs-based compound orders magnetically in three dimensions at $T_N = 1.85$ K [14,26]. The actual magnetic structure remains unknown to date, partially complicated by the unavailability of sufficiently large single crystals [26]. Preliminary unpublished powder neutron diffraction experiments suggest a magnetic propagation vector (0,0,0), which makes an accurate experimental determination exceedingly challenging. In applied magnetic fields it has a rather complex phase diagram, and achieves saturation at $\mu_0 H_c \sim 7.7$ T via a magnon-BEC-type QCP [26]. Inspired by the fact that the magnetic-field-induced AF phase in $Rb_2Cu_2Mo_3O_{12}$ is also ferroelectric (FE) [11,25,27], we performed detailed dielectric permittivity studies of $Cs_2Cu_2Mo_3O_{12}$ as a function of temperature (T), magnetic field (H) and probing frequency of the electric field (ω). To this end, we deposited conductive electrodes on opposing facets of a single crystal sample, such that the electric field was $\boldsymbol{E} \| \boldsymbol{c}^*$. The data were collected at dilution refrigerator temperatures in a capacitance bridge setup similar to that used in Ref. [11]. The change in complex capacitance was monitored as the external parameters and measurement frequency were varied. Experimental details are given in the Supplemental Material [28].

Raw capacitance data collected at $\omega = 1$ kHz are presented in Fig. 1. The real ($\Delta C'$) and imaginary ($\Delta C''$) components, proportional to the respective components of the dielectric constant ε' and ε'', are displayed in false colors as a function of temperature and magnetic field. At precisely the phase boundary separating the magnetically ordered and paramagnetic states (dashed line), $\Delta C'$ shows a sharp narrow peak, indicating the divergence of ε'.

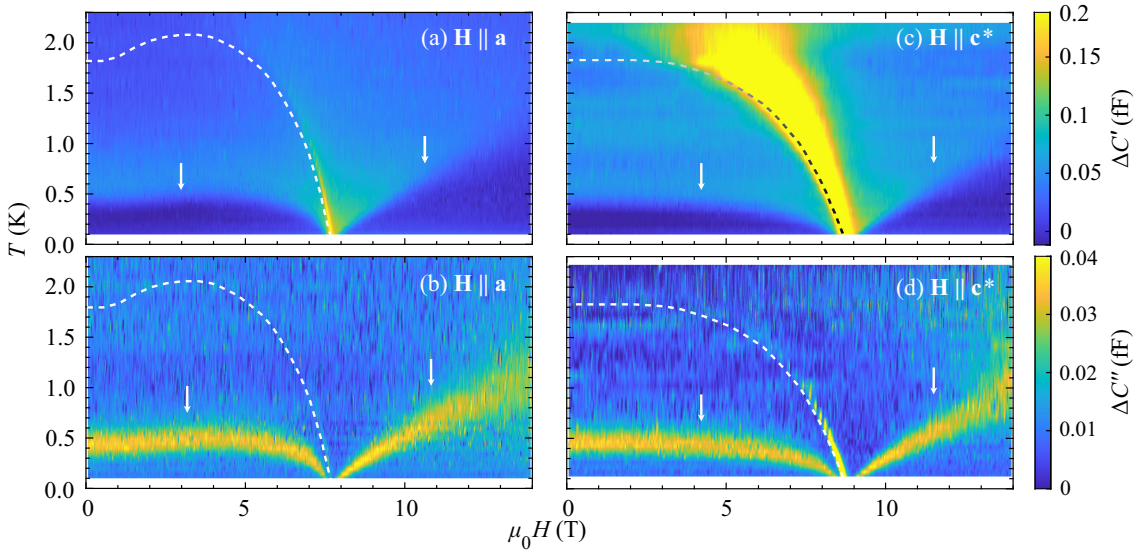

FIG. 1. False color plots of complex capacitance $\Delta C = \Delta C' + i\Delta C''$. The electric field is applied parallel to the $\boldsymbol{c}^*$ axis. The magnetic field is applied along two orthogonal crystallographic directions: (a),(b) $\boldsymbol{H}\|\boldsymbol{a}$ and (c),(d) $\boldsymbol{H}\|\boldsymbol{c}^*$. The color scale is shared across (a) and (c), and (b) and (d), respectively. It has been chosen to highlight the novel low temperature anomalies (arrows). As a result some stronger peaks at the magnetic phase boundary (dashed line, Ref. [26]) are blown out.

The magnitude of the anomaly is markedly different for $H\|a$ and $H\|c^*$ [28]. This feature is very similar to that previously seen in $Rb_2Cu_2Mo_3O_{12}$ [11]. The only obvious difference is that the Cs compound orders already in zero applied field, while its Rb-based counterpart is a quantum paramagnet and only shows spontaneous AF order when magnetized [24].

In both materials, this peak represents the onset of ferroelectricity simultaneous with magnetism in the ordered phase. As was previously done for the Rb-system [11], for $Cs_2Cu_2Mo_3O_{12}$ the appearance of spontaneous polarization was confirmed by pyroelectric current measurements (see Supplemental Material). Note that the dielectric constants of the two materials (see Fig. 4 in the Supplemental Material and Ref. [27]) are very close to one another at low temperatures, ruling out structural ferroelectricity driven by Cs substitution. Divergence of the capacitance implies that, along with any magnetic order, polarization is itself a primary order parameter of the transition, and is critical at the QCP at H_c [11]. This behavior is explained by the spin-current or inverse Dzyaloshinskii-Moriya mechanism of magnetoelectric coupling [9,29–31]. In this model $P \propto M_\perp M_\parallel$, the product of transverse staggered ($M_\perp$) and longitudinal uniform ($M_\parallel$) magnetization, respectively [11]. The former is the symmetry-breaking magnetic order parameter of the AF phase, while the latter is merely induced by the applied magnetic field. Consistently, no dielectric anomaly is found at the phase boundary at zero applied field, where no uniform magnetization is present. The strength of the anomaly increases as an external magnetic field progressively magnetizes the system.

The central new observation of the present study is an additional feature in the dielectric permittivity, one that has no analog in $Rb_2Cu_2Mo_3O_{12}$. In $Cs_2Cu_2Mo_3O_{12}$ it shows up as a broad peaklike feature in $\Delta C''(T)$ at temperatures well below T_c in the ordered phase. At fields above saturation it appears at a temperature that increases with applied field. It is accompanied by a rapid steplike change of $\Delta C'(T)$ (see Fig. 2 for details). Unlike the divergence at the phase boundary, these additional features show virtually no difference in magnitude between measurements under different magnetic field orientations (Fig. 1). Moreover, their magnitude is not particularly field-dependent, and they persist even in the absence of applied field. Obviously, their origin must be entirely different. Yet, both effects must be intimately linked, as they both coalesce and become critical at the QCP. We henceforth refer to the temperature at which $\Delta C''$ peaks as T^*. The values of T^* at different fields are displayed in Fig. 2 (triangles) and Fig. 4.

Several simple scenarios for the T^* feature can be ruled out. First, the feature must be a bulk- rather than a surface- or finite-size-effect since a comparable anomaly at the same T^* is also observed in polycrystalline samples [28]. Second, there is no thermodynamic phase transition at these temperatures [26]. Such a large dissipation is not something that one would expect at a thermodynamic phase transition. This is in contrast to the Rb-based compound [11], where the only dielectric anomaly observed corresponds precisely to the thermodynamic phase transition. A glasslike freezing transition at T^* is also unlikely, due to the absence of any hysteresis or history dependence in our measurements.

Steplike behavior of ε' above a magnetic-field-induced saturation QCP has been reported previously in another

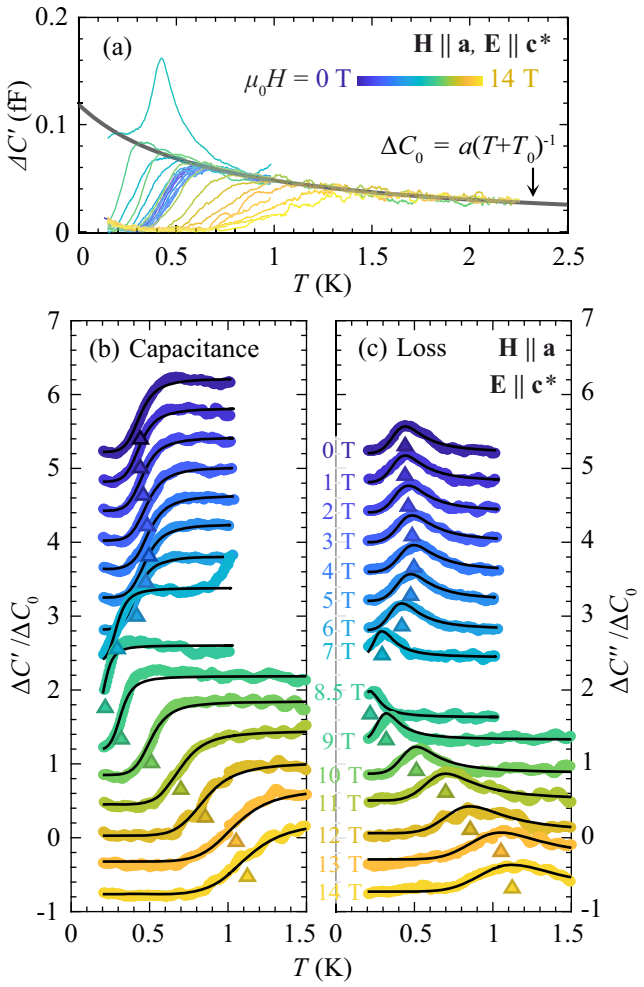

FIG. 2. Constant-field measurements of complex capacitance. (a) Regardless of the applied field, all capacitance curves collapse on a single line (solid black line) at elevated temperatures. The data shown in (b), real part, and (c), imaginary part, were normalized by the thus determined "background." The geometry corresponds to that of Figs. 1(a) and 1(b) $\boldsymbol{E}\|\boldsymbol{c}^*$ and $\boldsymbol{H}\|\boldsymbol{a}$. In all panels, same colors correspond to same magnetic field values. An offset of 0.4 units has been added between sets for visibility. Black solid lines show the best fit to the Cole-Cole model of Eq. (1). Note that both panels show the same scale and units. Shaded triangles denote the position of T^*.

quantum magnet $Ba_2CoGe_2O_7$ [6]. There it was attributed to the fluctuations of the AF order, the characteristic energy and temperature of the anomaly coinciding with that of the field-induced single-magnon Zeeman gap $g\mu_B\mu_0(H-H_c)$. This interpretation cannot be carried over to $Cs_2Cu_2Mo_3O_{12}$. In our material, above H_c the scale of T^* is roughly *ten times smaller* than the Zeeman gap (triangles vs the dashed line in Fig. 4). A different mechanism must be at play.

Since the data shown were collected at finite frequency of 1 kHz, one could suspect a proximity of a mechanical resonance in the measurement setup that couples to our probe. Frequency-dependent measurements firmly rule that out [28]: while some mechanical resonances are indeed detected, none are found in the immediate neighborhood of 1 kHz. Also, all appear to be excited by Lorentz forces in the connecting wires, and therefore vanish in the absence of an applied magnetic field, very much unlike the feature under discussion. The final suspicion is that slow dielectric relaxation may arise from trapping of charge carriers [32]. In our case this seems unlikely, as $Cs_2Cu_2Mo_3O_{12}$ is a good insulator and is transparent in bulk at room temperature.

The origin of the T^* feature is revealed in a quantitative analysis of the data. Noting the strong dissipative component, we attempted to fit the measurements with the phenomenological Cole-Cole model for dielectric relaxation [33,34]:

$$\Delta C = \frac{\Delta C_0(T)}{1+[i\omega\tau(T)]^{1-\alpha}}. \tag{1}$$

Here, $\Delta C_0(T)$ is proportional to the static dielectric constant $\varepsilon(T)$ and $\tau(T)$ is the relaxation time. The exponent $\alpha=0$ corresponds to the Debye relaxation model with a single relaxation time [35], while $\alpha<1$ accounts for a distribution of relaxation times within the solid.

Qualitatively, relaxation may be expected to occur faster at high temperature, and $\tau(T)$ is expected to decrease with increasing temperature. Therefore, at high enough T, ΔC Eq. (1) should be proportional to the static dielectric constant. In Fig. 2(a), we demonstrate that most of the measured $\Delta C'$ curves *collapse on a single, field-independent, line at* $T\gtrsim T^*$. The only exception is the data close to the QCP, where the sharp dielectric anomaly at the transition overwhelms the background. The resulting universal curve $\Delta C_0'(T)$ is well-fitted by the form $a(T+T_0)^{-1}$ [$T_0=0.68(1)$ K, Fig. 2(a)]. The lack of a field dependence of $\Delta C_0'(T)$ implies that this contribution is unrelated to magnetism and is entirely due to the crystal lattice. One could suspect the origin to be a yet undetected nearby structural transition, such as the one seen at around 20 K in $Rb_2Cu_2Mo_3O_{12}$ [11]. On the other hand, a lattice-driven ferroelectric transition is unlikely, due to the modest absolute value of the dielectric constant in $Cs_2Cu_2Mo_3O_{12}$ ($\epsilon\approx 5.5$, see Supplemental Material). Moreover, the relative change in the dielectric constant due to the temperature-dependent background is smaller than 1% [28]. We conclude that $\Delta C_0'(T)$ is due to some yet to be identified *persistent low-energy electric dipole degrees of freedom in* $Cs_2Cu_2Mo_3O_{12}$.

With $\Delta C_0'(T)$ characterized, the parameter α in Eq. (1) can be determined from the plots of the real vs imaginary parts of ΔC (Cole-Cole plots). As discussed in the Supplemental Material, the data *at all fields and temperatures* are well-described by *a single value*: $\alpha=0.2$. This supports Eq. (1) being an appropriate description. The only remaining fit parameter not determined globally is the characteristic timescale $\tau(T,H)$.

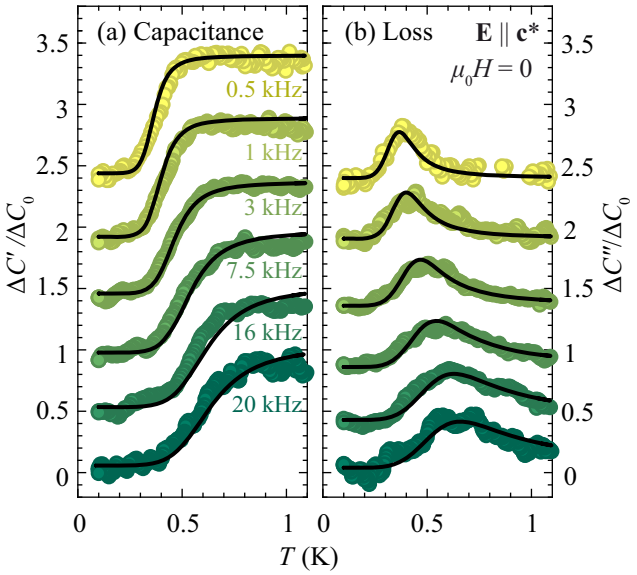

FIG. 3. Frequency dependence of complex capacitance at zero magnetic field: (a) real and (b) imaginary parts. The excitation frequency is consistently color-coded in the two panels. An offset of 0.5 units has been added for clarity. Black lines show the best fit to Eq. (1) with parameters fixed from Fig. 2.

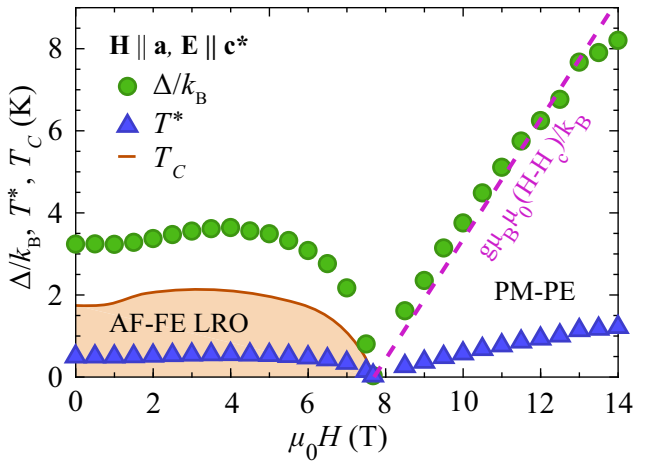

FIG. 4. Characteristic energy barrier extracted from Cole-Cole model (circles). Above the QCP, it follows the Zeeman energy of a single magnon, given by a pink dashed line. Triangles represent the position of T^*, at which the relaxing dissipative anomaly is observed. For completeness, the phase boundary is depicted, showing the PM-PE (paramagnetic-paraelectric) and AF-FE phases (shadowed) [26].

Except for the immediate proximity of QCP, at each value of magnetic field, excellent agreement with experiment is obtained assuming an activated behavior:

$$\tau(T,H) = \tau_0 \exp[\Delta(H)/k_B T]. \quad (2)$$

In this expression $\Delta(H)$ is the "barrier height" and τ_0 the "attempt time." The resulting fits are shown in Fig. 2. A *single field- and temperature-independent* $\tau_0 \approx 10^{-6}$ s was found to be sufficient to capture the data quantitatively. We have also checked that other values of τ_0 reduce the fit quality [28]. Note that *the real and imaginary parts are reproduced simultaneously* using the same values of $\Delta(H)$ for all temperatures. In contrast, if we were dealing with glassy behavior, relaxation times would be expected to show a divergent behavior at a finite temperature [34,36]. This is yet another argument against strong disorder effects and glassiness, despite the distribution of relaxation scales indicated by $\alpha = 0.2$.

Equation (1) implies a very specific form of frequency dependence. In Fig. 3 we demonstrate that the parameters extracted from the 1 kHz data also describe the capacitance measured at other frequencies ranging over more than a decade *without any additional fitting*. The conclusion is that the relaxation time $\tau(T,H)$ is *independent of probing frequency and is an intrinsic property of* $Cs_2Cu_2Mo_3O_{12}$.

The combined results of our Cole-Cole analysis are borne out in Fig. 4. The activation energy $\Delta(H)/k_B$ is shown alongside the temperature of long range ordering T_c [26] and T^*. Strikingly, for $H > H_c$, $\Delta(H)$ coincides with the single-magnon Zeeman gap $g\mu_B\mu_0(H - H_c)$, with $g = 2.16$ [24,25]. This strongly suggests that the T^* feature arises from the relaxation of low-energy structural dipole moments (the ones responsible for the background dielectric constant discussed above) by single magnons. The isotropy of T^* with respect to the field orientation naturally follows from the very isotropic g factor and saturation magnetization [26]. In the ordered phase, T^* does not change much at low fields, but goes to zero as $H \to H_c$. This behavior is also consistent with a single-magnon process within the ordered phase.

To put our findings in perspective, exponentially activated relaxation times are often observed in ferro- and paraelectrics [37–39]. In those cases, the activation energy usually corresponds to that of a longitudinal optical phonon [40]—an excitation carrying a finite dipole moment. In our case, though, the dielectric relaxation can be instead attributed to a magnon. This conclusively demonstrates that individual magnons can carry electric dipole moment in $Cs_2Cu_2Mo_3O_{12}$. Unlike the other cases of magnons showing electric behavior [41–47], the effects we observed persist beyond the ordered phase into the field polarized region $H > H_c$ and are detected at remarkably low temperatures and frequencies.

The obtained value of 10^{-6} s for the attempt time τ_0 in $Cs_2Cu_2Mo_3O_{12}$ is striking. It corresponds to a very low attempt frequency of 1 MHz. For most of the field range explored, the magnon frequency is of the order 0.1 THz, i.e., 5 orders of magnitude higher. This is in stark contrast to other polar insulators [37–39], where $\Delta\tau_0\hbar \sim 0.01$–$0.1$. The key difference is that in $Cs_2Cu_2Mo_3O_{12}$ the low-T dielectric response is likely coming from the lattice, while the relaxation is occurring by the spin excitations.

Therefore, τ_0 is determined by the strength of the spin-lattice coupling, which is expected to be much weaker than the phonon interactions in the ferroelectric case.

An interesting question is why the dielectric relaxation by magnons reported here for $Cs_2Cu_2Mo_3O_{12}$ is absent in a sister compound, $Rb_2Cu_2Mo_3O_{12}$. At high temperatures, crystal structures of these compounds are similar [15,24]. However, signatures of a structural change have been reported at about 20 K for $Rb_2Cu_2Mo_3O_{12}$ [24], suggesting that the crystalline structure may be important for dielectric relaxation. Dedicated future studies of crystalline and magnetic structure of $Cs_2Cu_2Mo_3O_{12}$ at low temperatures therefore may be able to clarify the microscopic origin of the dielectric relaxation by magnons.

In summary, we have demonstrated single-magnon relaxation of dielectric degrees of freedom in $Cs_2Cu_2Mo_3O_{12}$. The applied magnetic field becomes a convenient "knob" for tuning interactions between the polarizable lattice and spins due to proximity to a magnetic quantum critical point. These results open a new route to multiferroic quantum criticality [12] and potentially to coupling magnetic, electric, and optical degrees of freedom in hybrid quantum circuits [48,49].

This work is supported by a MINT grant of the Swiss National Science Foundation. P. C. is funded by DOE Basic Energy Sciences Grant DE-SC0020353 and P. A. V. was supported by a Rutgers Center for Materials Theory Abrahams Fellowship when this project was initiated. P. C. and P. A. V. acknowledge the Aspen Center for Physics where this work was discussed, which is supported by National Science Foundation Grant PHY-1607611 and a grant from the Simons Foundation (P. A. V.).

*Present address: Max-Planck-Institut für Festkörperforschung, Heisenbergstraße 1, 70569 Stuttgart, Germany.

†Present address: Dresden High Magnetic Field Laboratory (HLD-EMFL) and Würzburg-Dresden Cluster of Excellence ct.qmat, Helmholtz-Zentrum Dresden-Rossendorf, 01328 Dresden, Germany.

[1] E. G. Batyev and L. S. Braginski, Antiferromagnet in a strong magnetic field: Analogy with Bose gas, Sov. Phys. JETP **60**, 781 (1984), http://jetp.ras.ru/cgi-bin/dn/e_060_04_0781.pdf.

[2] T. Giamarchi and A. M. Tsvelik, Coupled ladders in a magnetic field, Phys. Rev. B **59**, 11398 (1999).

[3] T. Nikuni, M. Oshikawa, A. Oosawa, and H. Tanaka, Bose-Einstein Condensation of Dilute Magnons in $TlCuCl_3$, Phys. Rev. Lett. **84**, 5868 (2000).

[4] T. Giamarchi, C. Rüegg, and O. Tchernyshyov, Bose–Einstein condensation in magnetic insulators, Nat. Phys. **4**, 198 (2008).

[5] V. Zapf, M. Jaime, and C. D. Batista, Bose-Einstein condensation in quantum magnets, Rev. Mod. Phys. **86**, 563 (2014).

[6] J. W. Kim, S. Khim, S. H. Chun, Y. Jo, L. Balicas, H. T. Yi, S.-W. Cheong, N. Harrison, C. D. Batista, J. Hoon Han, and K. Hoon Kim, Manifestation of magnetic quantum fluctuations in the dielectric properties of a multiferroic, Nat. Commun. **5**, 4419 (2014).

[7] F. Schrettle, S. Krohns, P. Lunkenheimer, A. Loidl, E. Wulf, T. Yankova, and A. Zheludev, Magnetic-field induced multiferroicity in a quantum critical frustrated spin liquid, Phys. Rev. B **87**, 121105(R) (2013).

[8] K. Y. Povarov, A. Reichert, E. Wulf, and A. Zheludev, Giant dielectric nonlinearities at a magnetic Bose-Einstein condensation, Phys. Rev. B **92**, 140410(R) (2015).

[9] S. Kimura, K. Kakihata, Y. Sawada, K. Watanabe, M. Matsumoto, M. Hagiwara, and H. Tanaka, Ferroelectricity by Bose–Einstein condensation in a quantum magnet, Nat. Commun. **7**, 12822 (2016).

[10] S. Kimura, K. Kakihata, Y. Sawada, K. Watanabe, M. Matsumoto, M. Hagiwara, and H. Tanaka, Magnetoelectric effect in the quantum spin gap system $TlCuCl_3$, Phys. Rev. B **95**, 184420 (2017).

[11] S. Hayashida, L. Huberich, D. Flavián, Z. Yan, K. Y. Povarov, S. Gvasaliya, and A. Zheludev, Critical dielectric susceptibility at a magnetic BEC quantum critical point, Phys. Rev. Res. **3**, 033053 (2021).

[12] A. Narayan, A. Cano, A. V. Balatsky, and N. A. Spaldin, Multiferroic quantum criticality, Nat. Mater. **18**, 223 (2019).

[13] M. Hase, K. Ozawa, O. Suzuki, H. Kitazawa, G. Kido, H. Kuroe, and T. Sekine, Magnetism of $A_2Cu_2Mo_3O_{12}$ (A = Rb or Cs): Model compounds of a one-dimensional spin-1/2 Heisenberg system with ferromagnetic first-nearest-neighbor and antiferromagnetic second-nearest-neighbor interactions, J. Appl. Phys. **97**, 10B303 (2005).

[14] A. Fujimura, Y. Yasui, Y. Yanagisawa, I. Terasaki, Y. Kono, S. Kittaka, and T. Sakakibara, Comparison with ground states of frustrated quantum spin chain systems $A_2Cu_2Mo_3O_{12}$ (A = Rb and Cs), IEEE Trans. Magn. **52**, 1 (2016).

[15] The exact crystal structure of $Cs_2Cu_2Mo_3O_{12}$ was determined by single crystal x-ray diffraction as part of this work and is reported and discussed in the Supplemental Material. Previous discussions about the structure can also be found in [16–21].

[16] S. F. Solodovnikov and Z. A. Solodovnikova, New structure type in the morphotropic series of A^{2+} $M_2^{2+}(MoO_4)_3$: Crystal structure of $Rb_2Cu_2(MoO_4)_3$, J. Struct. Chem. **38**, 765 (1997).

[17] T. Hamasaki, H. Kuroe, T. Sekine, T. Naka, M. Hase, N. Maeshima, Y. Saiga, and Y. Uwatoko, Effects of high pressure on $A_2Cu_2Mo_3O_{12}$ (A = Rb, Cs): A one-dimensional system with competing ferromagnetic and antiferromagnetic interactions, J. Magn. Magn. Mater. **310**, e394 (2007).

[18] Y. Hoshino, S. Atarashi, T. Goto, M. Hase, and T. Sasaki, Ground state of the competing spin chain $Cs_2Cu_2Mo_3O_{12}$, JPS Conf. Proc. **3** 014012 (2014).

[19] T. Goto, A. Yagi, K. Matsui, I. Watanabe, T. Sasaki, and M. Hase, NMR and μ-SR study on competing Heisenberg chain $Cs_2Cu_2Mo_3O_{12}$, J. Phys. Conf. Ser. **828**, 012017 (2017).

[20] A. Yagi, K. Matsui, T. Goto, M. Hase, and T. Sasaki, ^{133}Cs-NMR study on aligned powder of competing spin

chain compound $Cs_2Cu_2Mo_3O_{12}$, J. Phys. Conf. Ser. **969**, 012125 (2018).
[21] K. Matsui, T. Goto, J. Angel, I. Watanabe, T. Sasaki, and M. Hase, Ground state of quasi-one dimensional competing spin chain $Cs_2Cu_2Mo_3O_{12}$ at zero and finite fields, JPS Conf. Proc. **21** 011008 (2018).
[22] M. Hase, H. Kuroe, K. Ozawa, O. Suzuki, H. Kitazawa, G. Kido, and T. Sekine, Magnetic properties of $Rb_2Cu_2Mo_3O_{12}$ including a one-dimensional spin-1/2 Heisenberg system with ferromagnetic first-nearest-neighbor and antiferromagnetic second-nearest-neighbor exchange interactions, Phys. Rev. B **70**, 104426 (2004).
[23] Y. Yasui, R. Okazaki, I. Terasaki, M. Hase, M. Hagihala, T. Masuda, and T. Sakakibara, Low temperature magnetic properties of frustrated quantum spin chain system $Rb_2Cu_2Mo_3O_{12}$, J. Phys. Soc. Jpn. Conf. Proc. **3**, 014014 (2014).
[24] S. Hayashida, D. Blosser, K. Y. Povarov, Z. Yan, S. Gvasaliya, A. N. Ponomaryov, S. A. Zvyagin, and A. Zheludev, One- and three-dimensional quantum phase transitions and anisotropy in $Rb_2Cu_2Mo_3O_{12}$, Phys. Rev. B **100**, 134427 (2019).
[25] H. Ueda, S. Onoda, Y. Yamaguchi, T. Kimura, D. Yoshizawa, T. Morioka, M. Hagiwara, M. Hagihala, M. Soda, T. Masuda, T. Sakakibara, K. Tomiyasu, S. Ohira-Kawamura, K. Nakajima, R. Kajimoto, M. Nakamura, Y. Inamura, N. Reynolds, M. Frontzek, J. S. White, M. Hase, and Y. Yasui, Emergent spin-1 Haldane gap and ferroelectricity in a frustrated spin-$\frac{1}{2}$ ladder, Phys. Rev. B **101**, 140408(R) (2020).
[26] D. Flavián, S. Hayashida, L. Huberich, D. Blosser, K. Y. Povarov, Z. Yan, S. Gvasaliya, and A. Zheludev, Magnetic phase diagram of the linear quantum ferro-antiferromagnet $Cs_2Cu_2Mo_3O_{12}$, Phys. Rev. B **101**, 224408 (2020).
[27] N. Reynolds, A. Mannig, H. Luetkens, C. Baines, T. Goko, R. Scheuermann, L. Keller, M. Bartkowiak, A. Fujimura, Y. Yasui, C. Niedermayer, and J. S. White, Magnetoelectric coupling without long-range magnetic order in the spin-$\frac{1}{2}$ multiferroic $Rb_2Cu_2Mo_3O_{12}$, Phys. Rev. B **99**, 214443 (2019).
[28] See Supplemental Material at http://link.aps.org/supplemental/10.1103/PhysRevLett.130.216501 for further details.
[29] H. Katsura, N. Nagaosa, and A. V. Balatsky, Spin Current and Magnetoelectric Effect in Noncollinear Magnets, Phys. Rev. Lett. **95**, 057205 (2005).
[30] M. Mostovoy, Ferroelectricity in Spiral Magnets, Phys. Rev. Lett. **96**, 067601 (2006).
[31] Y. Tokura, S. Seki, and N. Nagaosa, Multiferroics of spin origin, Rep. Prog. Phys. **77**, 076501 (2014).
[32] N. Ng, R. Ahluwalia, A. Kumar, D. J. Srolovitz, P. Chandra, and J. F. Scott, Electron-beam driven relaxation oscillations in ferroelectric nanodisks, Appl. Phys. Lett. **107**, 152902 (2015).
[33] K. S. Cole and R. H. Cole, Dispersion and absorption in dielectrics I. Alternating current characteristics, J. Chem. Phys. **9**, 341 (1941).
[34] F. Kremer and A. Schönhals, *Broadband Dielectric Spectroscopy* (Springer Science & Business Media, New York, 2002).
[35] P. J. W. Debye, *Polar Molecules* (Dover publications, New York, 1929), 10.1002/jctb.5000484320.
[36] B. E. Vugmeister and M. D. Glinchuk, Dipole glass and ferroelectricity in random-site electric dipole systems, Rev. Mod. Phys. **62**, 993 (1990).
[37] O. Bidault, P. Goux, M. Kchikech, M. Belkaoumi, and M. Maglione, Space-charge relaxation in perovskites, Phys. Rev. B **49**, 7868 (1994).
[38] R. Viana, P. Lunkenheimer, J. Hemberger, R. Böhmer, and A. Loidl, Dielectric spectroscopy in $SrTiO_3$, Phys. Rev. B **50**, 601 (1994).
[39] C. Ang, J. F. Scott, Z. Yu, H. Ledbetter, and J. L. Baptista, Dielectric and ultrasonic anomalies at 16, 37, and 65 k in $SrTiO_3$, Phys. Rev. B **59**, 6661 (1999).
[40] J. F. Scott, Comment on the physical mechanisms of the 37 K and 65 K anomalies in strontium titanate, J. Phys. Condens. Matter **11**, 8149 (1999).
[41] A. Pimenov, A. Mukhin, V. Y. Ivanov, V. Travkin, A. Balbashov, and A. Loidl, Possible evidence for electromagnons in multiferroic manganites, Nat. Phys. **2**, 97 (2006).
[42] A. Pimenov, A. M. Shuvaev, A. A. Mukhin, and A. Loidl, Electromagnons in multiferroic manganites, J. Phys. Condens. Matter **20**, 434209 (2008).
[43] V. N. Krivoruchko, Electrically active magnetic excitations in antiferromagnets (Review Article), Low Temp. Phys. **38**, 807 (2012).
[44] T. N. Stanislavchuk, Y. Wang, Y. Janssen, G. L. Carr, S.-W. Cheong, and A. A. Sirenko, Magnon and electromagnon excitations in multiferroic $DyFeO_3$, Phys. Rev. B **93**, 094403 (2016).
[45] A. Pimenov, A. Loidl, A. A. Mukhin, V. D. Travkin, V. Y. Ivanov, and A. M. Balbashov, Terahertz spectroscopy of electromagnons in $Eu_{1-x}Y_xMnO_3$, Phys. Rev. B **77**, 014438 (2008).
[46] N. Kida, Y. Ikebe, Y. Takahashi, J. P. He, Y. Kaneko, Y. Yamasaki, R. Shimano, T. Arima, N. Nagaosa, and Y. Tokura, Electrically driven spin excitation in the ferroelectric magnet $DyMnO_3$, Phys. Rev. B **78**, 104414 (2008).
[47] C. P. Grams, D. Brüning, S. Kopatz, T. Lorenz, P. Becker, L. Bohatý, and J. Hemberger, Observation of chiral solitons in $LiCuVO_4$, Commun. Phys. **5**, 1 (2022).
[48] D. Lachance-Quirion, Y. Tabuchi, A. Gloppe, K. Usami, and Y. Nakamura, Hybrid quantum systems based on magnonics, Appl. Phys. Express **12**, 070101 (2019).
[49] A. Clerk, K. Lehnert, P. Bertet, J. Petta, and Y. Nakamura, Hybrid quantum systems with circuit quantum electrodynamics, Nat. Phys. **16**, 257 (2020).